Holmberg, Nico; Laasonen, Kari

Theoretical Insight into the Hydrogen Evolution Activity of Open-Ended Carbon Nanotubes

Published in:
Journal of Physical Chemistry Letters

DOI:
10.1021/acs.jpclett.5b01846

Published: 01/01/2015

Document Version
Peer-reviewed accepted author manuscript, also known as Final accepted manuscript or Post-print

Published under the following license:
Unspecified

Please cite the original version:
Holmberg, N., & Laasonen, K. (2015). Theoretical Insight into the Hydrogen Evolution Activity of Open-Ended Carbon Nanotubes. *Journal of Physical Chemistry Letters*, *6*(19), 3956-3960.
https://doi.org/10.1021/acs.jpclett.5b01846

J. Phys. Chem. Lett., 2015, 6 (19), pp 3956–3960, DOI: 10.1021/acs.jpclett.5b01846

Theoretical Insight into the Hydrogen Evolution Activity of Open-Ended Carbon Nanotubes

Nico Holmberg and Kari Laasonen*

COMP Centre of Excellence in Computational Nanoscience, Department of Chemistry, Aalto University, P.O. Box 16100, FI-00076 Aalto, Finland

E-mail: kari.laasonen@aalto.fi

Abstract

Carbon nanotubes (CNTs), while inactive by themselves, are often used as a platform in the search of new catalysts for the hydrogen evolution reaction (HER) by introducing metal nanoparticles or other dopants. Here, we examine the HER activity of pristine open-ended CNTs considering both the effects of chirality and hydrogen coverage using electronic structure calculations. The results indicate that the formation of different 5-ring structures at the end of the CNT introduces surface sites that are highly active towards HER, whereas the activity of traditional 6-ring sites is not greatly altered by tube termination. At fixed hydrogen coverage, the enhanced activity of these sites was attributed to valence orbitals residing close to the highest occupied molecular level facilitating electron transfer to protons.

Graphical TOC Entry

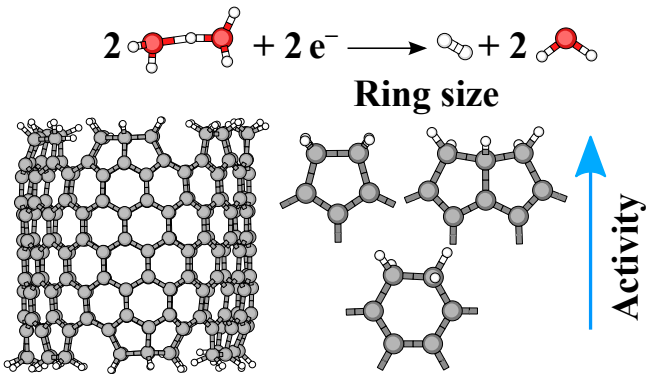

Keywords

density functional theory, nudged elastic band method, hydrogen evolution reaction, electrocatalysis, ring size effect, proton-coupled electron transfer

Carbon-based catalysts are an attractive class of materials for the hydrogen evolution reaction (HER) due to their versatility and the abundance of carbon. The catalytic activity of pure carbon compounds, such as nanotubes (CNTs) or graphene, is however insufficient for practical applications. Common strategies to enhance activity include doping with other nonmetals, e.g. nitrogen or sulfur,[1,2] functionalizing carbon with for instance acidic groups,[3] or adding metal-rich nanoparticles either by decorating[4–7] or encapsulating[8–11] them, to name just a few possibilities.

Density functional theory (DFT) simulations have deepened our fundamental understanding of HER on transition metals exemplified by studies ranging from characterizing elementary reaction steps on Pt,[12] binary alloy screening,[13] and to explaining the electronic origins of HER activity.[14] By contrast, the number of studies[15–18] exploring HER on carbon-based materials remains scarce and there is no theory motivated consensus on, for example, which dopants contribute to HER activity. In this Letter, we consider pristine open-ended CNTs and demonstrate how the reactivity of carbon can be tuned by the formation of 5-ring structures.

Figure 1 shows the studied open-ended CNT model systems which depending on tube chirality become terminated by a mixture of carbon 5-rings and fused 5-rings, or by 6-rings following a geometry optimization in the presence of hydrogen. To assess how hydrogen binds to different surface sites, which are labeled according to Figure 1, vacuum adsorption energies were calculated for different surface hydrogen coverages using the methodology detailed in the Supporting Information with calculated values presented in Tables S1-S2. Additionally, total projected density of states are given in Figure S1 for the considered surface sites, demonstrating that each site type introduces electronic states near the Fermi level of the CNTs but that the phenomenon is more pronounced on the 5-rings. Regardless of surface site, adsorption energies are strongly correlated with the distribution adsorbed hydrogen atoms near the surface site. Two opposite effects are present: direct neighbors decrease adsorption energies while neighbors two C-C bonds distant increase them. The effects also

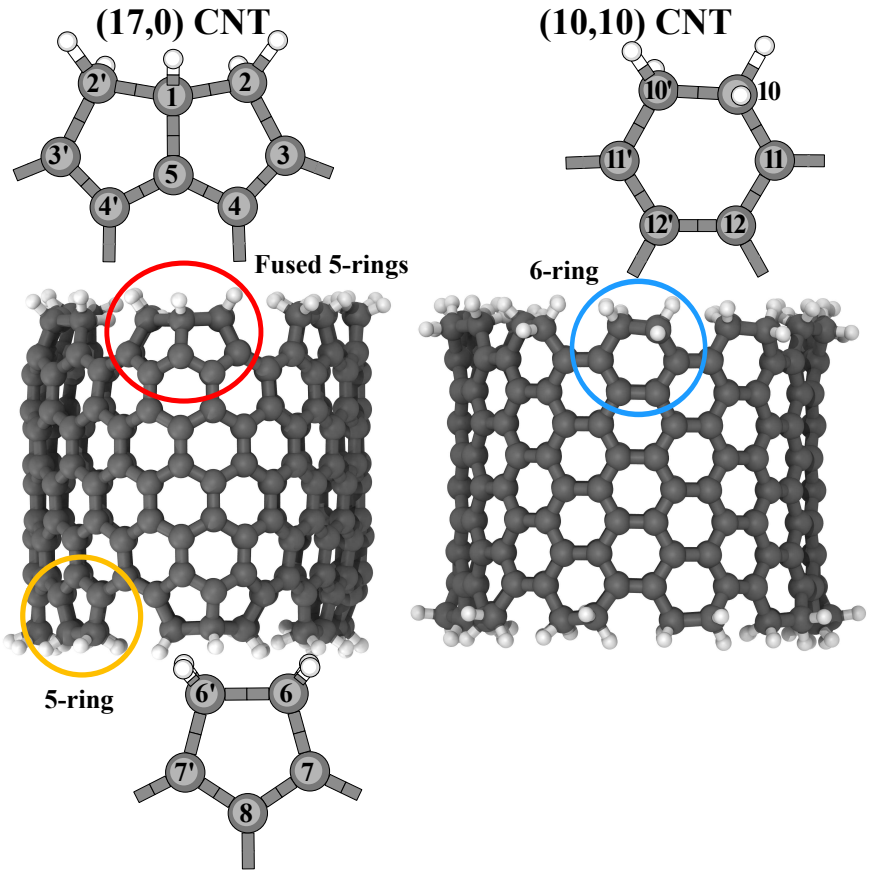

Figure 1. Investigated model systems of open-ended CNTs. The $(17, 0)$ CNT is terminated on both sides by a mixture of carbon 5-rings and fused 5-rings, while the $(10, 10)$ CNT is terminated solely by 6-rings. Reaction sites are labeled according to the insets with the addition that the site between any 5-rings is labeled **9**. Due to symmetry, primed and unprimed sites are expected to be equally reactive and are considered as a single site type.

extend to adjacent rings on the edge of the open-ended CNTs. Identical behavior has been reported for pristine CNTs[18] allowing us to predict which configurations are HER active. Specifically, configurations with large, positive adsorption energies should be most reactive towards the Heyrovsky step ($H^+ + e^- + H^* \rightarrow H_2$) of HER, while the reverse should hold for the Volmer reaction ($H^+ + e^- \rightarrow H^*$). Thus, maximizing HER activity requires both steps to be balanced. In this Letter, we consider only the Volmer-Heyrovsky mechanism of HER, since testing revealed that the Tafel reaction ($2H^* \rightarrow H_2$) is improbable due to substantially (> 2 eV) higher activation energies for investigated hydrogen coverages (see Table S4), in agreement with prior results.[15,16,18]

In order to thoroughly explore the HER reactivity of open-ended CNTs as a function of hydrogen coverage, 2-3 configurations with distinctly different adsorption energies were selected and nudged elastic band[19] calculations were performed to identify transition states along the individual steps of HER. The calculated reaction and activation energies are presented in Table S3 of the Supporting Information. Here, we focus on equivalent corner sites $\mathbf{3}, \mathbf{7}', \mathbf{11}'$ in different ring terminations of the open-ended CNTs since preliminary screening indicates these sites to be the most active, at least on the 5-ring terminated CNT. The effect of ring size on HER activation energies is illustrated in Figure 2 where linear fits (see Figure S2) to the calculated barriers against adsorption energy are presented. Here, we wish to note that an analysis based on adsorption free energies would yield identical results, as we have previously[18] shown that vibrational contributions to free energy are within 0.1 eV on different carbon sites regardless of coverage so that free energies are obtained by applying a constant shift of ~ 0.35 eV to the calculated adsorption energies.

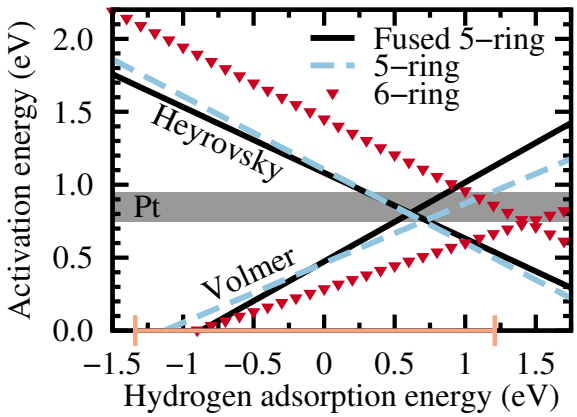

Figure 2. Effect of ring size on HER activation energies on corner sites $\mathbf{3}, \mathbf{7}', \mathbf{11}'$ in the studied open-ended CNTs. Activation energies vary with the distribution of adsorbed hydrogens near the active site, as distinguished by vacuum adsorption energies. The range of observed adsorption energies on the 5-ring is denoted by the colored segment on the x-axis. For comparison, the computational HER barrier on flat Pt(111) at fixed 0.86 monolayer hydrogen coverage, 0.85 eV,[12] is included with standard 0.1 eV error bars.

Both sites in the 5-ring structures exhibit similar HER activation energies with the maximum barrier being decidedly lower than in the 6-ring. For a wide range of configurations, the barrier is in fact on the same order as the computational HER barrier on a flat Pt(111)

surface[12] under fixed hydrogen coverage conditions at the thermodynamic redox potential of HER. In addition, we find that the correlations for both reactions on the 6-ring coincide with similar relations[18] obtained for a pristine (14,0) CNT, especially in the region of maximum activity near the intercept point of the two graphs. Interestingly, the Volmer barriers on the 6-ring are lower than on either 5-ring structure, while the reverse holds and the difference is amplified for the Heyrovsky reaction. This suggests that the 6-ring site has a tendency to overbind hydrogen, which ultimately might lead to a decreased catalytic performance compared to the 5-rings. To gauge the HER activity of open-ended CNTs, full energy diagrams need to be constructed using the evaluated activation and reaction energies. While the present data suggests the 6-ring is the most active when only the edge sites are occupied (see highlighted entries in Table S3), this configuration is expected to be improbable as filling additional corner sites remains exothermic. Instead, Figure 3 shows a comparison of HER energy diagrams in two configurations where the occupancy of sites closest to edge sites is varied (see Figure S3) with an additional comparison presented in Figure S4.

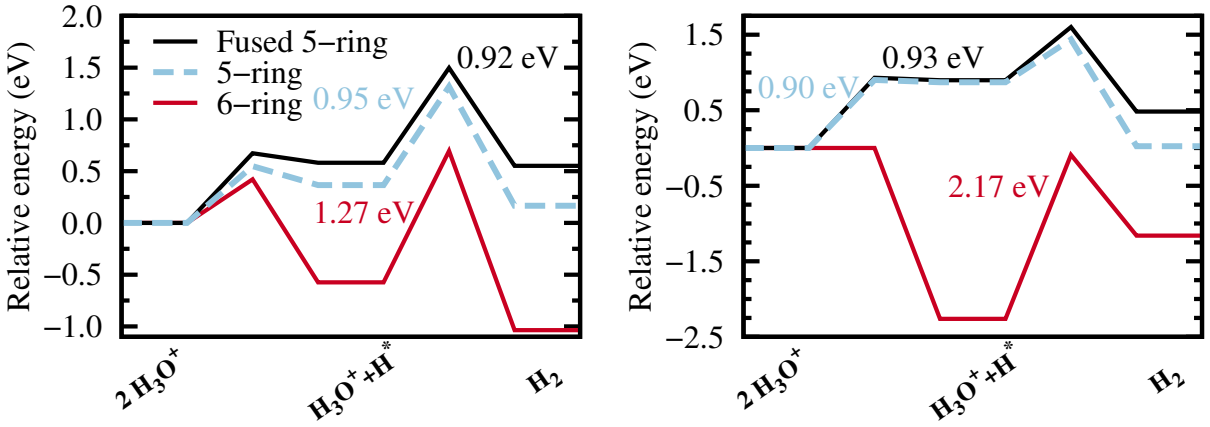

Figure 3. Comparison of HER activity on corner sites in fused 5-rings, 5-rings and 6-rings terminating the studied open-ended CNTs. At left, all sites closest to the inert edge of the rings are occupied; at right, the same sites in the closest adjacent ring relative to the active site are also occupied. Effective HER barriers are indicated.

As before, the effective HER barriers on the 5-ring sites are virtually identical and lower than on the 6-ring. The major difference between ring sizes is the fact that corner sites in 6-rings are directly linked, both readily becoming occupied, which increases the barrier of

the Heyrovsky step dramatically. In the 5-rings, it is energetically less favorable to fill sites adjacent to the corner sites and their effect on HER activity is less profound, increasing barriers only by $0.3 - 0.4$ eV (see Figure S4). We wish to emphasize that the presented Volmer barriers are upper bounds because they are calculated for reactions where the distribution of adsorbed hydrogens near the active site remains fixed, whereas Scheme S1 in the Supporting Information demonstrates that a different filling order would lead to a smaller effective barrier. This example illustrates a typical limitation of computational modeling where surface coverage can often only be included as a static quantity instead of as a true, dynamical variable, which is also influenced by external quantities such as solution pH and electrode potential. However, as Figures 2-3 demonstrate, establishing coverage dependent scaling relations is a successful and mandatory strategy to realistically compare the reactivity of surface sites in carbon-based nanomaterials. Moreover, seeing as many reaction paths with sub eV barriers can be constructed, it can be concluded that the computational HER activity of 5-ring corner sites exceeds that of pristine CNTs with barriers reported in the range $1.1 - 1.2$ eV (zero coverage)[16,18] and is even comparable to Pt(111).[12]

To gain insight into the origins of reactivity in carbon 5-rings, it is necessary to go beyond energetic considerations and to examine electronic effects. Indeed, on transition metal surfaces, active HER catalysts have been demonstrated to fulfill three criteria: they have a d-band spanning the Fermi level, the band has strong long-range interactions with the empty proton $1s$ orbital necessary for electron transfer, and the adsorption of hydrogen is thermoneutral ($\Delta G \approx 0$).[14] In spirit of the d-band model, Zheng et al.[17] studied doped graphene clusters and measured the distance between active site valence orbitals and cluster Fermi energy within the framework of natural bond orbitals. Contrary to observations on metals, the authors showed hydrogen adsorption energies became more exothermic with increasing distance to Fermi energy implying a growth in HER activity, assuming only thermoneutrality is required to maximize reaction rate. The validity of this assumption is difficult to assess given experimental limitations in preparing samples of required purity. Further-

more, since there is no apparent correlation between adsorption energies and HER barriers in the current (see Figure S5) and previous studies,[15,18] we introduce a similar orbital energy dependent descriptor ΔE but instead relate it directly to calculated HER barriers. Specifically, for each site j, the distance between the system's highest occupied molecular orbital (HOMO), depicted in Figure 4, and the occupancy $q_{i\sigma}$ weighed average orbital energy ε is measured according to

$$\Delta E_j = \varepsilon^{\mathrm{IBO}}_{\mathrm{HOMO}} - \frac{1}{\sum q_{i\sigma}} \sum_{\sigma=\uparrow,\downarrow} \sum_i q_{i\sigma} \varepsilon^{\mathrm{IBO}}_{i\sigma} \tag{1}$$

The final, site-type specific quantity is obtained after averaging over all similar sites on one side of the open-ended CNT. Here, atom-centered orbitals are obtained with the intrinsic bond orbital (IBO) localization scheme.[20] The relationship between ΔE and HER barriers is explored in Figure 5. This comparison is performed for reactions modeled on open-ended CNTs with the edge fully hydrogenated i.e. at the (improbable) low coverage limit, since inclusion of coverage effects is far from trivial (see discussion below).

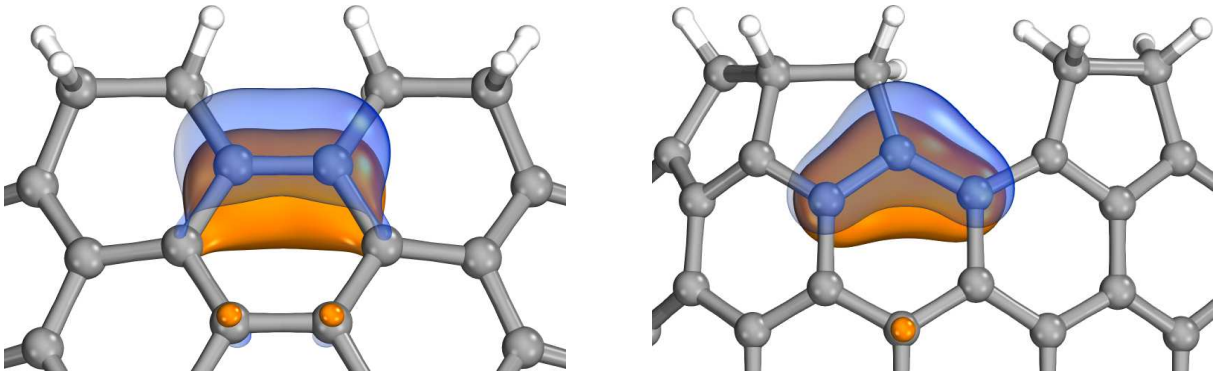

Figure 4. Highest occupied molecular orbitals of the open-ended $(10, 10)$ (left) and $(17, 0)$ (right) CNTs visualized using the intrinsic bond orbital localization method. The isosurfaces enclose 70 % of the orbital's electron density.[21]

On the open-ended $(17, 0)$ CNT, site specific HER activity increases linearly the closer the valence orbitals are to the HOMO energy level. Upon changing the chirality, this relationship vanishes becoming essentially flat, though there are only two distinct site types. Notably, the valence orbitals of both investigated 6-ring sites reside deep below the highest state.

Comparing corner sites in different rings, the IBOs of both 5-ring structures are closer in energy to the HOMO and they are more strongly localized on the corner atom than in the 6-ring. This suggests that ring strain is the root cause for the differentiation in HER reactivity on surface sites in the 5-rings. Under the given hydrogen coverage conditions at least, this effect correlates directly with the splitting of valence orbital energy levels leading to the dependence observed in Figure 5. Furthermore, the observation that valence states closest to the HOMO level are the most active indicates that the reactivity of corner sites can actually be attributed to an enhanced coupling with the empty proton 1s state–a result agreeing with proposed reactivity theories on transition metals.[14] At the same time, all sites in the 6-ring appear to be roughly equivalent and, in fact, HER barriers on these sites match the value obtained for a pristine CNT of the same chirality at zero hydrogen coverage.[16]

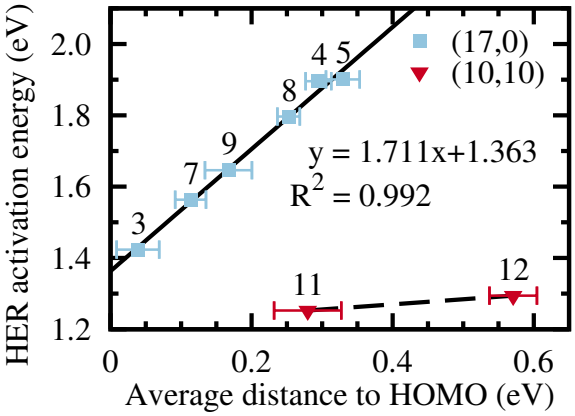

Figure 5. HER activation energies on different surface sites of the investigated open-ended CNTs plotted against the average distance between the system HOMO and the reactive orbitals of the site (Equation 1). The solid line is a linear fit to the $(17, 0)$ data with fit indicated, whereas the dashed line serves as a guide to the eye. Standard deviation has been used as the error estimate.

While the introduced descriptor ΔE allows us to successfully predict the relative reactivity ordering of surface sites on the open-ended $(17, 0)$ CNT, and to a lesser degree on the $(10, 10)$ CNT, it remains uncertain whether the predictive power of this quantity can be extended to arbitrary hydrogen coverages, given the computational challenge of evaluating the necessary number of HER barriers and deciding which adsorption configurations are even

comparable with each other. Certainly, we expect the ordering of sites and both the slope and position of the relationship to change with coverage. Perhaps what is most unsatisfying, however, is the finding that this descriptor does not permit comparison of different tube chiralities, since the CNTs remain incomparable even when the 0.16 eV difference in the position of the HOMO is taken into consideration. Further work is therefore clearly needed to understand reactivity trends in carbon nanomaterials.

In summary, electronic structure calculations were used to assess the HER activity of open-ended CNTs under varying hydrogen coverage conditions. Depending on tube chirality, the CNTs became terminated either by 6-rings or a mixture of 5-rings and fused 5-rings, with corner sites in the last two structures exhibiting considerable activity towards HER. Unlike surface sites in the 6-ring, significant asymmetry in the reactivity of sites in the 5-rings was discovered. For a fixed hydrogen coverage, this observation was explained by demonstrating that sites with valence orbitals closest to the HOMO energy level were catalytically the most active. These findings suggest that pristine carbon is not as inert as is commonly thought and that the introduction of different ring structures might lead to enhanced HER activity not only in open-ended CNTs but also in e.g. fullerenes or carbon nanobuds.[22] Experimental verification of these findings will however require adjusting synthesis techniques to maximize the concentration of active 5-ring sites.

Computational Methods

Density functional theory calculations were performed within the hybrid Gaussian and planewaves framework using the CP2K/Quickstep[23] code. The PBE[24] functional was used for the exchange-correlation interaction and van der Waals interactions were included with the DFT-D3 method.[25] The $2s$ and $2p$ orbitals of C and O and the $1s$ orbital of H were treated as valence states, which were expanded in molecularly optimized Gaussian basis sets of double-ζ plus polarization quality.[26] Nonlinear core corrected Goedecker-Teter-Hutter

pseudopotentials were employed for the ionic cores.[27] The auxiliary planewave basis was truncated with a 550 Ry kinetic energy cutoff.

The investigated open-ended $(10, 10)$ (containing 200 carbon atoms) and $(17, 0)$ (204 carbon atoms) CNTs were placed in vacuum inside a cubic cell with 4.3 nm edge length and interactions between periodic copies of the system were removed in all directions by the Martyna-Tuckerman method.[28] HER activation and reaction energies were evaluated using the climbing image nudged elastic band method[19] using 8/12 images (Volmer/Heyrovsky) and an 0.1 eV/Å maximum force convergence criterion. Vibrational analysis was used to confirm that the transition states contained only a single imaginary frequency and these are given in the Supporting Information, Table S3. Solvation effects were included by enclosing the reacting Zundel cation inside a 15 water molecule shell, as illustrated in the Supporting Information, Figure S6. Only the Zundel cation and carbon atoms in rings closest to the active site were allowed to move during NEB. Intrinsic bond orbital[20] analysis was carried out with the IboView[29] program. The analysis was performed on wavefunctions that were optimized with the ORCA[30] code using the def2-TZVP primary basis and the corresponding Coulomb-fitting basis.[31]

Acknowledgement

This study was financed by the Academy of Finland through its Centres of Excellence Program, project no. 251748. N.H. is supported by Aalto University School of Chemical Technology through a PhD scholarship. Computational resources were provided by CSC–the Finnish IT Centre for Science.

Supporting Information Available

Additional details regarding the computational methodology; Figures S1-S6; Tables S1-S4; Scheme S1. This material is available free of charge via the Internet at `http://pubs.acs.`

org/.

References

(1) Zheng, Y.; Jiao, Y.; Zhu, Y.; Li, L. H.; Han, Y.; Chen, Y.; Du, A.; Jaroniec, M.; Qiao, S. Z. Hydrogen Evolution by a Metal-Free Electrocatalyst. *Nat. Commun.* **2014**, *5*, 3738.

(2) Ito, Y.; Cong, W.; Fujita, T.; Tang, Z.; Chen, M. High Catalytic Activity of Nitrogen and Sulfur Co-Doped Nanoporous Graphene in the Hydrogen Evolution Reaction. *Angew. Chem. Int. Ed.* **2015**, *54*, 2131–2136.

(3) Cui, W.; Liu, Q.; Cheng, N.; Asiri, A. M.; Sun, X. Activated Carbon Nanotubes: A Highly-Active Metal-Free Electrocatalyst for Hydrogen Evolution Reaction. *Chem. Commun.* **2014**, *50*, 9340–9342.

(4) Li, Y.; Wang, H.; Xie, L.; Liang, Y.; Hong, G.; Dai, H. MoS_2 Nanoparticles Grown on Graphene: An Advanced Catalyst for the Hydrogen Evolution Reaction. *J. Am. Chem. Soc.* **2011**, *133*, 7296–7299.

(5) Yan, Y.; Ge, X.; Liu, Z.; Wang, J.-Y.; Lee, J.-M.; Wang, X. Facile Synthesis of Low Crystalline MoS_2 Nanosheet-Coated CNTs for Enhanced Hydrogen Evolution Reaction. *Nanoscale* **2013**, *5*, 7768–7771.

(6) Liu, Q.; Tian, J.; Cui, W.; Jiang, P.; Cheng, N.; Asiri, A. M.; Sun, X. Carbon Nanotubes Decorated with CoP Nanocrystals: A Highly Active Non-Noble-Metal Nanohybrid Electrocatalyst for Hydrogen Evolution. *Angew. Chem. Int. Ed.* **2014**, *53*, 6710–6714.

(7) Jin, H.; Wang, J.; Su, D.; Wei, Z.; Pang, Z.; Wang, Y. In situ Cobalt–Cobalt Oxide/N-Doped Carbon Hybrids as Superior Bifunctional Electrocatalysts for Hydrogen and Oxygen Evolution. *J. Am. Chem. Soc.* **2015**, *137*, 2688–2694.

(8) Zou, X.; Huang, X.; Goswami, A.; Silva, R.; Sathe, B. R.; Mikmeková, E.; Asefa, T. Cobalt-Embedded Nitrogen-Rich Carbon Nanotubes Efficiently Catalyze Hydrogen Evolution Reaction at All pH Values. *Angew. Chem. Int. Ed.* **2014**, *53*, 4372–4376.

(9) Tavakkoli, M.; Kallio, T.; Reynaud, O.; Nasibulin, A. G.; Johans, C.; Sainio, J.; Jiang, H.; Kauppinen, E. I.; Laasonen, K. Single-Shell Carbon-Encapsulated Iron Nanoparticles: Synthesis and High Electrocatalytic Activity for Hydrogen Evolution Reaction. *Angew. Chem. Int. Ed.* **2015**, *54*, 4535–4538.

(10) Gao, S.; Li, G.-D.; Liu, Y.; Chen, H.; Feng, L.-L.; Wang, Y.; Yang, M.; Wang, D.; Wang, S.; Zou, X. Electrocatalytic H_2 Production from Seawater over Co, N-Codoped Nanocarbons. *Nanoscale* **2015**, *7*, 2306–2316.

(11) Liang, H.-W.; Bruller, S.; Dong, R.; Zhang, J.; Feng, X.; Mullen, K. Molecular Metal-Nx Centres in Porous Carbon for Electrocatalytic Hydrogen Evolution. *Nat. Commun.* **2015**, *6*, 7992.

(12) Skúlason, E.; Tripkovic, V.; Björketun, M. E.; Gudmundsdóttir, S.; Karlberg, G.; Rossmeisl, J.; Bligaard, T.; Jónsson, H.; Nørskov, J. K. Modeling the Electrochemical Hydrogen Oxidation and Evolution Reactions on the Basis of Density Functional Theory Calculations. *J. Phys. Chem. C* **2010**, *114*, 18182–18197.

(13) Greeley, J.; Jaramillo, T. F.; Bonde, J.; Chorkendorff, I.; Nørskov, J. K. Computational High-Throughput Screening of Electrocatalytic Materials for Hydrogen Evolution. *Nat. Mater.* **2006**, *5*, 909–913.

(14) Santos, E.; Quaino, P.; Schmickler, W. Theory of Electrocatalysis: Hydrogen Evolution and More. *Phys. Chem. Chem. Phys.* **2012**, *14*, 11224–11233.

(15) Deng, J.; Ren, P.; Deng, D.; Yu, L.; Yang, F.; Bao, X. Highly Active and Durable Non-Precious-Metal Catalysts Encapsulated in Carbon Nanotubes for Hydrogen Evolution Reaction. *Energy Environ. Sci.* **2014**, *7*, 1919–1923.

(16) Das, R. K.; Wang, Y.; Vasilyeva, S. V.; Donoghue, E.; Pucher, I.; Kamenov, G.; Cheng, H.-P.; Rinzler, A. G. Extraordinary Hydrogen Evolution and Oxidation Reaction Activity from Carbon Nanotubes and Graphitic Carbons. *ACS Nano* **2014**, *8*, 8447–8456.

(17) Zheng, Y.; Jiao, Y.; Li, L. H.; Xing, T.; Chen, Y.; Jaroniec, M.; Qiao, S. Z. Toward Design of Synergistically Active Carbon-Based Catalysts for Electrocatalytic Hydrogen Evolution. *ACS Nano* **2014**, *8*, 5290–5296.

(18) Holmberg, N.; Laasonen, K. Ab Initio Electrochemistry: Exploring the Hydrogen Evolution Reaction on Carbon Nanotubes. *J. Phys. Chem. C* **2015**, *119*, 16166–16178.

(19) Henkelman, G.; Uberuaga, B. P.; Jónsson, H. A Climbing Image Nudged Elastic Band Method for Finding Saddle Points and Minimum Energy Paths. *J. Chem. Phys.* **2000**, *113*, 9901–9904.

(20) Knizia, G. Intrinsic Atomic Orbitals: An Unbiased Bridge between Quantum Theory and Chemical Concepts. *J. Chem. Theory Comput.* **2013**, *9*, 4834–4843.

(21) Lehtola, S.; Jónsson, H. Pipek–Mezey Orbital Localization Using Various Partial Charge Estimates. *J. Chem. Theory Comput.* **2014**, *10*, 642–649.

(22) Nasibulin, A. G.; Pikhitsa, P. V.; Jiang, H.; Brown, D. P.; Krasheninnikov, A. V.; Anisimov, A. S.; Queipo, P.; Moisala, A.; Gonzalez, D.; Lientschnig, G. et al. A Novel Hybrid Carbon Material. *Nat. Nanotechnol.* **2007**, *2*, 156–161.

(23) (a) VandeVondele, J.; Krack, M.; Mohamed, F.; Parrinello, M.; Chassaing, T.; Hutter, J. Quickstep: Fast and Accurate Density Functional Calculations Using a Mixed Gaussian and Plane Waves Approach. *Comput. Phys. Commun.* **2005**, *167*, 103–128; (b) Hutter, J.; Iannuzzi, M.; Schiffmann, F.; VandeVondele, J. CP2K: Atomistic Simulations of Condensed Matter Systems. *Wiley Interdiscip. Rev.: Comput. Mol. Sci.* **2014**, *4*, 15–25.

(24) Perdew, J. P.; Burke, K.; Ernzerhof, M. Generalized Gradient Approximation Made Simple. *Phys. Rev. Lett.* **1996**, *77*, 3865–3868.

(25) Grimme, S.; Antony, J.; Ehrlich, S.; Krieg, H. A Consistent and Accurate Ab Initio Parametrization of Density Functional Dispersion Correction (DFT-D) for the 94 Elements H-Pu. *J. Chem. Phys.* **2010**, *132*, 154104–19.

(26) VandeVondele, J.; Hutter, J. Gaussian Basis Sets for Accurate Calculations on Molecular Systems in Gas and Condensed Phases. *J. Chem. Phys.* **2007**, *127*, 114105–9.

(27) Willand, A.; Kvashnin, Y. O.; Genovese, L.; Vázquez-Mayagoitia, Á.; Deb, A. K.; Sadeghi, A.; Deutsch, T.; Goedecker, S. Norm-Conserving Pseudopotentials with Chemical Accuracy Compared to All-Electron Calculations. *J. Chem. Phys.* **2013**, *138*, 104109.

(28) Martyna, G. J.; Tuckerman, M. E. A Reciprocal Space Based Method for Treating Long Range Interactions in Ab Initio and Force-Field-Based Calculations in Clusters. *J. Chem. Phys.* **1999**, *110*, 2810–2821.

(29) (a) Knizia, G.; Klein, J. E. M. N. Electron Flow in Reaction Mechanisms–Revealed from First Principles. *Angew. Chem. Int. Ed.* **2015**, *54*, 5518–5522; (b) Knizia, G. IboView - A Program for Chemical Analysis. `http://www.iboview.org/`, Accessed: July 14, 2015.

(30) Neese, F. The ORCA Program System. *Wiley Interdiscip. Rev.: Comput. Mol. Sci.* **2012**, *2*, 73–78.

(31) (a) Weigend, F.; Ahlrichs, R. Balanced Basis Sets of Split Valence, Triple Zeta Valence and Quadruple Zeta Valence Quality for H to Rn: Design and Assessment of Accuracy. *Phys. Chem. Chem. Phys.* **2005**, *7*, 3297–3305; (b) Weigend, F. Accurate Coulomb-fitting Basis Sets for H to Rn. *Phys. Chem. Chem. Phys.* **2006**, *8*, 1057–1065.